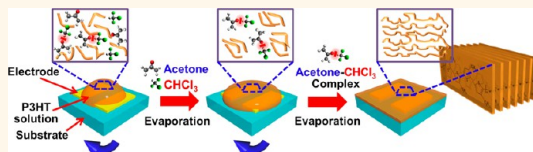


Solvent Based Hydrogen Bonding: Impact on Poly(3-hexylthiophene) Nanoscale Morphology and Charge Transport Characteristics

Mincheol Chang,[†] Dalsu Choi,[†] Boyi Fu,[†] and Elsa Reichmanis^{†,‡,§,*}

[†]School of Chemical and Biomolecular Engineering, [‡]School of Chemistry and Biochemistry, [§]School of Materials Science and Engineering, Georgia Institute of Technology, Atlanta, Georgia 30332-0100, United States

ABSTRACT We demonstrate that supramolecular assembly and subsequent enhancement of charge transport characteristics of conjugated polymers can be facilitated simply by adding small amounts of a more volatile poor solvent, which can hydrogen bond with the majority solvent. Addition of up to 2 vol % acetone to a precursor solution of poly(3-hexylthiophene) (P3HT) in chloroform leads to approximately a 4-fold increase in P3HT field-effect mobility. The improvement is associated with hydrogen bonding interactions between acetone and chloroform which decrease the evaporation rate of the mixed solvent. P3HT is less soluble in the binary solvent than in the more readily vaporized chloroform component, and this characteristic enables the supramolecular assembly of P3HT chains at the nanoscale. Two-dimensional molecular ordering of the polymer film was controlled by varying the quantity of poor solvent added to the precursor solution, and the correlation between field-effect mobility and molecular ordering was investigated. Hansen solubility parameters were used to systematically understand how the solvent mixture enhances the alignment and assembly of polymer chains and influences subsequent thin film properties. The value of the relative energy difference (RED) of the solvent with respect to P3HT increased from less than 1 to more than 1 during film formation, which indicates that the solvent characteristics are initially those of a good solvent but transform into those of a poor dissolution medium. A mechanistic illustration of the molecular ordering process during film formation is postulated.



KEYWORDS: hydrogen bonding · solvent mixtures · π – π stacking · poly(3-hexylthiophene) · supramolecular assembly · organic field effect transistors · Hansen solubility parameters

Conjugated polymer semiconductors have attracted great interest due to their low-temperature, solution-based processability, which may provide for low-cost, large-area electronic device fabrication.^{1–6} While significant advances have been made, polymeric semiconducting materials are disadvantaged because of relatively low field-effect mobilities owing to the relatively low degree of polymer thin-film crystallinity.^{7–9} Solution processed conjugated polymer films are typically semicrystalline, composed of many small crystalline regions embedded within a largely disordered matrix. This thin-film architecture impedes efficient charge hopping between transport sites.^{7–9}

Poly(3-hexylthiophene) (P3HT) is a representative conjugated polymer that has been investigated for device applications due to its hole transporting properties, solubility in a range of organic solvents, and good

film-forming properties.^{10–17} Molecular parameters such as polymer molecular weight (MW) and regioregularity (RR) have been studied as means to control thin-film microstructure and resultant electrical properties.^{16,18–20} It was proposed that for higher MW material, the longer chain length enhances macroscopic charge transport because (i) intramolecular charge transport through longer conjugated segments becomes favorable over interchain hopping, and (ii) the longer chains connect crystalline domains that are separated by low conductivity amorphous regions.^{18,19} Further, it was suggested that mobility increases as the RR increases because of an increase in the charge hopping rate due to reduced reorganization energies and a reduction in the number of grain boundaries as a result of wider nanofibrils.¹⁶

In addition to modification of molecular parameters, process modifications have also

* Address correspondence to ereichmanis@chbe.gatech.edu.

Received for review March 15, 2013 and accepted May 7, 2013.

Published online May 07, 2013
10.1021/nn401323f

© 2013 American Chemical Society

been explored for achieving thin-film morphologies commensurate with efficient charge transport.^{13,15,21–27} Parameters such as solvent boiling point,²⁷ postdeposition processing (thermal or solvent vapor annealing),^{13,23} solution preparation method (sonication)^{21,24} and conjugated polymer solubility^{15,25} have been shown to impact the supramolecular self-assembly of the π -conjugated materials. For example, Sirringhaus *et al.* reported that use of high boiling point solvents helps promote formation of highly self-ordered microcrystalline structures in P3HT, thus significantly improving P3HT field effect mobility relative to that obtained from lower boiling point alternatives (*ca.* 10^{-1} vs 10^{-2} $\text{cm}^2 \text{ V}^{-1} \text{ s}^{-1}$).²⁷ It was theorized that the higher boiling point limits solvent evaporation from the polymer matrix and thus increases the time available for crystallization during the spin-coating process. Lee *et al.* demonstrated that annealing P3HT at high temperature ($\sim 150^\circ \text{C}$) increases polymer crystallinity and improves contact between the semiconductor and device electrodes, affording an increase,¹³ while Tsai *et al.* showed that molecular ordering of P3HT chains was enhanced upon exposure of the polymer film to *o*-dichlorobenzene vapor.²³ Order of magnitude improvements in P3HT mobility can also be achieved by the solution preparation method. Aiyar *et al.* reported that ultrasonic irradiation of P3HT solutions promotes π -stacking induced molecular aggregation, which effects an increase in mobility.²¹

However, the approaches described above have limitations that may be undesirable for large-scale fabrication and high-throughput processing. The use of high boiling point solvents requires additional high temperature treatment to remove residual solvent after thin-film deposition. Thermal annealing could give rise to deformation of a flexible, low glass transition temperature substrate, or risk degradation of the semiconducting polymer itself, and solvent vapor annealing might present safety concerns.^{28–31} The ultrasonic irradiation process requires immersion of the solution into a bath, presenting its own set of scale-up challenges.

Approaches that do not require a post-treatment to improve molecular ordering and charge transport in polymer semiconductors which use poor solvents have recently been reported.^{15,32–34} A poor solvent having a boiling point higher than that of the main solvent induced formation of ordered aggregates of polymer semiconductors during solvent evaporation. The less volatile poor solvent resides within the evolving film for a longer period of time and thus promotes aggregation. For example, Cho *et al.* reported that addition of the higher boiling non-solvent acetonitrile (bp 81°C) to a precursor solution of P3HT in chloroform (bp 61°C) led to enhanced two-dimensional ordering of P3HT chains and concomitant charge transport characteristics.¹⁵ No post-treatment steps were required; the nonsolvent is believed to promote formation of ordered P3HT aggregates during

deposition *via* spin coating.¹⁵ The same report emphasized that use of a lower boiling point poor solvent has no impact on the structure and morphology of resultant P3HT thin-films.¹⁵ Thus, higher volatility poor solvents with respect to the majority component have not been investigated for inducing well-ordered π -conjugated polymer aggregates even though they present many favorable attributes with regard to processing thin-films.^{35–40}

Here, we demonstrate that a higher volatility solvent that additionally interacts with the majority solvent through hydrogen bonding leads to enhanced supramolecular assembly of P3HT, a representative π -conjugated polymer semiconductor. Two-dimensional molecular ordering of the conjugated polymer film is controlled by varying the “poor” to “good” solvent ratio. A correlation between the molecular ordering of P3HT chains and resultant charge transport characteristics as measured by the field-effect mobility is demonstrated. Hydrogen bonding interactions between the main solvent and minority poor solvent are investigated by analysis of the evaporation rates and spectroscopic properties of the solvent mixtures and individual components. Hansen solubility parameters, including the dispersive solubility parameter (δ_D), the polar solubility parameter (δ_D) and the H-bonding solubility parameter (δ_H) of the polymer and solvent mixtures are used to understand how the binary solvent can enhance polymer supramolecular assembly and subsequently, the macroscopic charge transport characteristics of resultant thin-films. A mechanistic illustration of the polymer chain molecular ordering process is presented.

The approach described here utilizes fundamental principles and presents quantitative insights that could facilitate identification of solvent systems applicable to polymer semiconductor processing for electronic devices. Extension to organic–organic blends or organic–inorganic nanocomposites can be envisioned. The mechanistic approach using Hansen solubility parameters enhances understanding of the evolution of the nano- through macroscale morphology of solution processed polymer π -conjugated polymer materials and further, the complex relationship between materials morphology and charge transport characteristics.

RESULTS AND DISCUSSION

The effect of solvent–solvent and solvent–solute interactions on the optical properties, nano- through macro-structure, and charge transport characteristics of solidified P3HT thin-films were evaluated using alternative deposition solvents comprised of a “good”/“poor” solvent blend. Chloroform (bp 61°C) and chlorobenzene (bp 131°C) were used as representative good solvents for the polythiophene (solubility >10 mg/mL), and are among the most commonly used solvents for π -conjugated polymer semiconductor processing.^{25,26,41} Two poor solvents, both

of which are relatively volatile, were selected. P3HT exhibits poor solubility (solubility less than 0.1 mg/mL) in acetone and 2,3-dimethylbutane which have similar boiling points (56 °C vs 58 °C, respectively),^{25,26,41} and should have no impact on P3HT final thin-film morphology or charge transport characteristics.¹⁵ The “poor” solvents were selected because they are volatile, with similar evaporation rates, and yet they have widely different polarities. While the substituted butane is a nonpolar hydrocarbon, acetone is a polar solvent that readily interacts with other moieties through hydrogen bonding. The chloroform/acetone system in particular is one of the most studied C–H···O hydrogen-bonded complexes (see Supporting Information).^{42–46}

Solutions of P3HT were prepared in either chloroform or chlorobenzene, and to avoid macroscopic aggregation of P3HT, the concentration of poor solvent was limited to less than 5 vol %. At higher proportions of poor solvent, the polymer precipitates, forming large aggregates which carry through to the solidified thin-films and lead to poor macroscopic charge transport.¹⁵ Bottom contact field-effect transistors (FETs) were fabricated by spin coating as-prepared P3HT solutions onto prefabricated device substrates. Figure 1a shows the impact of an increase in poor solvent concentration on the mobility of resultant semiconducting polymer films. The average mobility was calculated in the saturation regime of transistor operation ($V_{DS} = -80$ V) by plotting the drain current (I_{DS}) versus gate voltage (V_{GS}) and fitting the data to the following eq 1:⁴⁷

$$I_{DS} = \frac{WC_{OX}}{2L} \mu (V_{GS} - V_T)^2 \quad (1)$$

where W (2000 μ m) and L (50 μ m) are the transistor channel width and length, respectively, V_T is the threshold voltage and C_{OX} is the capacitance per unit area of the silicon dioxide gate dielectric (1.15×10^{-8} F/cm 2).

P3HT mobility gradually increases from 4.3×10^{-3} to 1.7×10^{-2} cm 2 V $^{-1}$ s $^{-1}$ for thin-films prepared from solutions of chloroform with increases in acetone concentration up to 2 vol % (Figure 1a). The mobility observed here is similar to that reported for P3HT where 3.3 vol % of a high boiling poor solvent was used to enhance the crystallinity and electrical performance of P3HT films (1.5×10^{-2} cm 2 V $^{-1}$ s $^{-1}$),¹⁵ and is about a factor of 4 greater than that of P3HT prepared via spin coating from chloroform solution (4.3×10^{-3} cm 2 V $^{-1}$ s $^{-1}$). Rapid evaporation of chloroform during the spin coating process leads to relatively poor molecular ordering of the polymer chains with commensurately lower macroscopic mobility.^{15,16,48} Addition of acetone as a cosolvent is believed to enhance P3HT molecular ordering resulting in improved charge carrier transport characteristics. Increasing the concentration of acetone from 2 to 5 vol % effects a decrease in mobility (Figure 1a) which is attributed to inhomogeneity

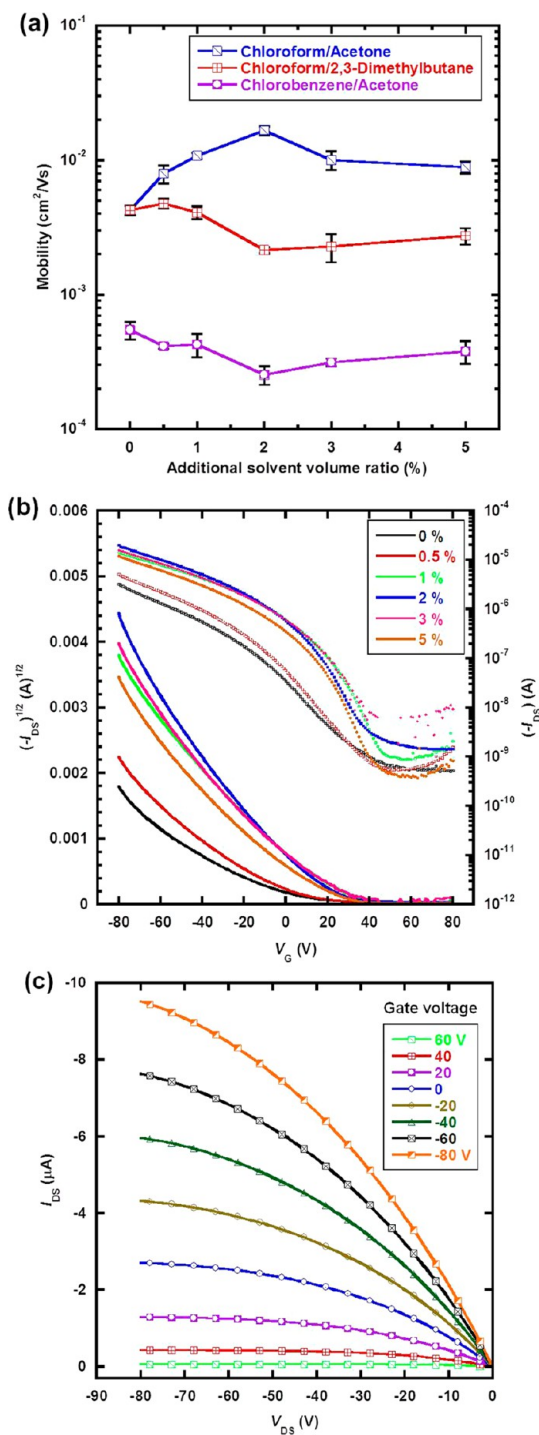


Figure 1. (a) Average field-effect mobilities obtained from P3HT films obtained via spin coating from chloroform/acetone, chloroform/2,3-dimethylbutane and chlorobenzene/acetone solvent blends having a range of poor solvent volume ratios. Mobilities were calculated in the saturation regime of operation with $V_D = -80$ V. (b) Transfer characteristics of P3HT OFETs fabricated using chloroform/acetone blends. (c) Typical output characteristics obtained from a P3HT OFET prepared via spin coating from chloroform/acetone where the acetone content is 2 vol %. All measurements were performed in a nitrogen glovebox.

of the resultant P3HT films,¹⁵ while the increased concentration of poor solvent may enhance the degree of

molecular ordering and crystallinity of the polymer thin-films,¹⁵ it may lead to an increase in the number of interfaces between crystalline domains thus preventing efficient charge transport.

In contrast to the results obtained with the chloroform/acetone solvent system, neither the chloroform/2,3-dimethylbutane nor chlorobenzene/acetone blends noticeably impact P3HT charge transport properties. Rather, they provide results that are similar to those of P3HT films prepared from the respective single component solvents, chloroform and chlorobenzene. Figure 1b, c exhibits transfer and output characteristic curves which are typical of p-channel OFET operation in the accumulation mode. The high turn-on voltages (V_{ON}) apparent in Figure 1b are attributed to the effects of residual doping and/or acceptor-like traps at the P3HT–oxide interface.⁴⁹ Spectroscopic and morphological studies of P3HT prepared using these same solvent systems also presented no substantive differences in comparison to results obtained from the single component solvents (see Supporting Information).

Figure 2 depicts the electronic absorption spectra obtained from P3HT/chloroform–acetone solution and the corresponding semiconductor thin-films. The absorption maximum, λ_{max} , associated with the $\pi-\pi^*$ intraband transition, appears at *ca.* 450 nm for all solutions, while absorption bands associated with a vibronic structure having a 0–0 transition at *ca.* 610 nm and a vibronic side band at *ca.* 570 nm are noticeably absent (Figure 2a).^{50,51} Thus, addition of the poor solvent, acetone, with volume ratios below 5% relative to chloroform, does not appear to effect aggregation of the P3HT chains in solution.

In contrast to the solution results, P3HT thin-films obtained from chloroform/acetone blends display clearly different spectral features in comparison to the pristine film, as shown in Figure 2b. The band appearing at *ca.* 533 nm sequentially red-shifts as the concentration of acetone increases. Additionally, weak absorption bands begin to develop at lower energies (λ *ca.* 555 and 605 nm), indicative of vibronic structure originating from improved co-facial π -stacking of P3HT.⁵² These features are attributed to enhanced planarization and thus, effective conjugation length of the polymer main chain. Addition of acetone to solutions of P3HT in chloroform appears to promote that planarization resulting in improved molecular ordering of P3HT chains through $\pi-\pi$ stacking.

Enhanced intermolecular interactions between P3HT chains are expected to give rise to films that are more crystalline.⁵³ Figure 3 shows the X-ray diffractograms obtained from grazing incidence (GIXD) measurements of P3HT films obtained from the chloroform/acetone solutions. As shown in Figure 3a, increases in poor solvent concentration effects a gradual increase in intensity of the (100) peak associated with lamellar packing of the polymer chains along the crystallographic

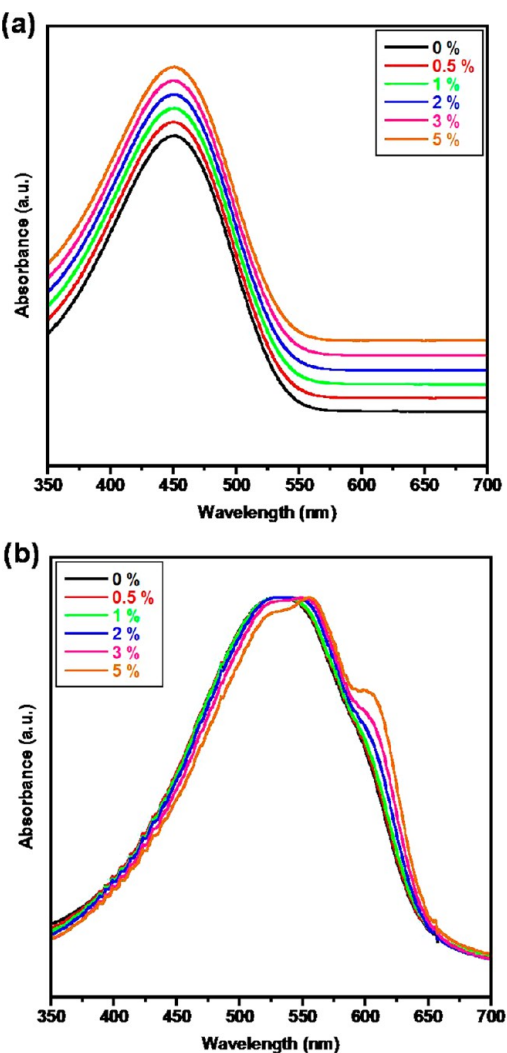


Figure 2. Normalized UV–visible absorption spectra of (a) P3HT/chloroform–acetone solutions with differing volume ratios of acetone to chloroform, and (b) the corresponding P3HT thin-films obtained by spin coating. The spectra obtained from the solutions were shifted for better comparison.

direction perpendicular to the backbone.⁵⁴ This increase could be attributed to either an increase in the size of individual crystallites, the number of crystallites, or both.²¹ Also, the (100) peak gradually shifts to higher angle, from 5.22 to 5.41°, when the acetone volume ratio is increased from 0 to 5 vol %, indicating that the *d*-spacing in the (100) plane decreases from 16.91 to 16.31 Å (Figure 3b). This decrease may result from increased interdigitation between the P3HT alkyl side chains, or a change in side chain tilt because of unfavorable solvent–solute interactions as poor solvent is incorporated into the system.^{34,55}

Atomic Force Microscopy (AFM) was used to investigate the surface morphologies of P3HT thin-films prepared from 0, 0.5, 1, 2, 3, and 5 vol % chloroform/acetone solutions. Phase and height images are presented in Figure 4, where P3HT thin-film nano- and microstructure distinctively evolves from an initial featureless and amorphous structure as the acetone

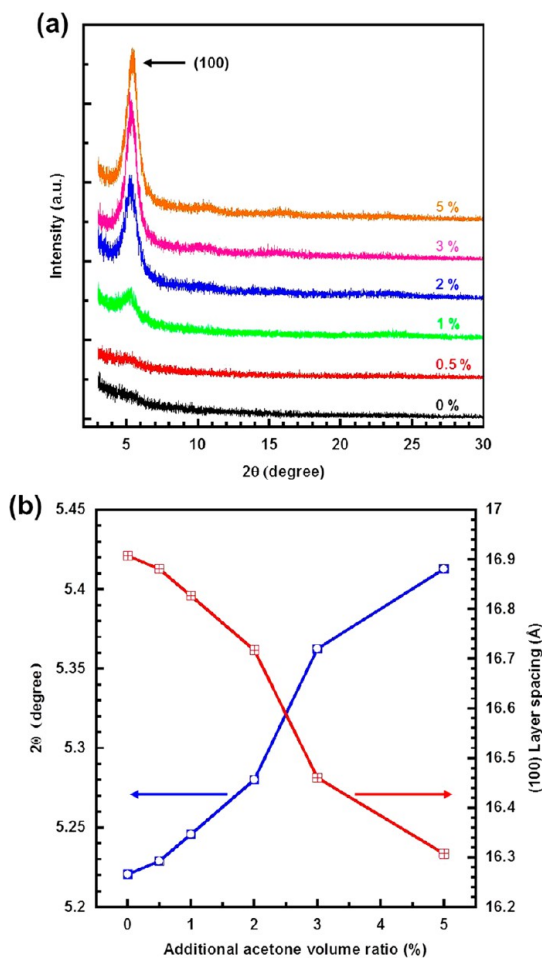


Figure 3. (a) Grazing incidence X-ray diffraction profiles of P3HT films spin-coated from P3HT/chloroform solutions containing a range of added acetone. (b) 2θ angle (left axis) of (100) peak and corresponding layer spacing (right axis) as a function of the additional acetone volume ratio.

content increases. Consistent with previous reports, rapid evaporation of chloroform during the coating process hinders formation of well-ordered, supramolecular structures.^{21,27} Using the binary chloroform/acetone solvent system, randomly shaped, nanosized grains begin to appear, and then increase in size, as the volume ratio of acetone increases. Addition of the poor solvent appears to induce supramolecular assembly of the P3HT chains either in solution and/or during the coating process.

Concomitant with assembly/alignment of P3HT chains is an increase in long-range lateral order, expected to be beneficial for efficient charge transport.^{14,40} The observed increase in field-effect mobility upon addition of up to 2 vol % acetone is consistent with this expectation. However, as seen from the height images, when the proportion of acetone is greater than 2 vol %, both grain size and surface roughness increase significantly. Thus, the interfaces between grains become more resistive to charge transport because interconnectivity is lacking, and the corresponding field-effect mobility decreases (Figure 1a).

From the results presented above, blends of a relatively good solvent with a poor solvent can afford

markedly different results with respect to charge transport characteristics. Demonstrably, use of a poor solvent able to interact with the majority solvent through hydrogen bonding can enhance the supramolecular assembly of π -conjugated polymer chains and thus positively influence the charge transport characteristics of the resultant film. Specifically, blends of chloroform and acetone, which are known to hydrogen bond with each other, lead to molecular alignment and ordering at the nanoscale affording a macroscopic thin-film structure conducive to efficient charge transport. From a mechanistic perspective, it is important to understand how such small percentages of a poor solvent additive can promote molecular ordering and thereby transport. We hypothesize that solvent–solvent (majority “good” solvent–minority “poor” solvent) and subsequently, solvent–solute (solvent mixture–P3HT) interactions promote aggregation and favorable π – π stacking between the P3HT chains. In the chloroform–acetone system, hydrogen bonding interactions lead to formation of a solvent complex that persists in the evolving thin-film for a longer time than either individual “free” component due to a lower evaporation rate of the complex. Concomitantly, polymer solubility decreases, perhaps gradually, as the concentration of complexed solvent increases, thereby promoting favorable π – π stacking interactions between the polymer chains, thus enhancing solidified film charge transport characteristics.^{15,56}

At ambient temperature, hydrogen bonding effects a decrease in the evaporation rate of a chloroform/acetone blend as the acetone volume ratio increases from 0 to ca. 33 vol %.⁴² The change in evaporation rate of the blended solvent in P3HT/solvent solutions was investigated as a function of acetone volume fraction. In agreement with expectations, the evaporation rate decreases as the acetone volume ratio is increased to 5 vol % (see Supporting Information).⁴² FT-IR spectroscopy confirmed the presence of hydrogen bonding between the two solvent components (see Supporting Information).^{57,58} Given that the volatility of the chloroform/acetone system is minimized at ca. 33 vol %, it is anticipated that the volume ratio of acetone to chloroform in the P3HT/solvent systems investigated here would converge to ca. 33 vol % during evaporation; the more volatile fractions will exit first, leaving behind a more acetone rich binary solvent regardless of the starting chloroform–acetone ratio.

Solvents are known to affect the growth of organic crystals in a significant manner.^{15,32} Similarly, the organization of polymer based semiconductors into assemblies that are conducive to effective macroscopic charge carrier transport has also been shown to be sensitive to the solvent environment. Use of a poor solvent allows polymer chains to aggregate, thus minimizing unfavorable solute–solvent interactions and facilitating molecular ordering between polymer chains through favorable π – π stacking. A factor that is expected to be useful to aid

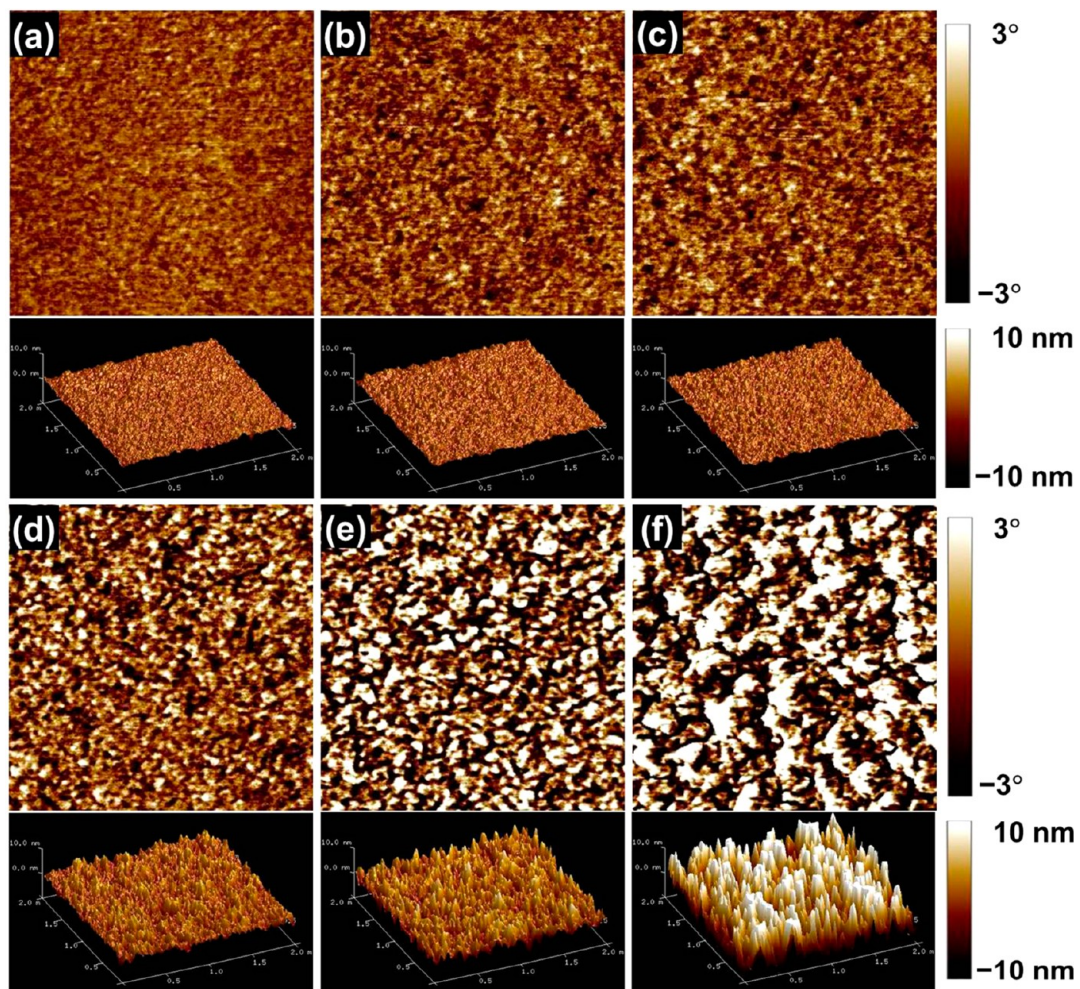


Figure 4. Tapping mode AFM phase (upper) and height images (lower) of P3HT films obtained *via* spin-casting from chloroform/acetone solution; the P3HT films were fabricated from solutions containing (a) 0, (b) 0.5, (c) 1, (d) 2, (e) 3, and (f) 5 vol % acetone. The scan area of phase and height images is $1\text{ }\mu\text{m} \times 1\text{ }\mu\text{m}$ and $2\text{ }\mu\text{m} \times 2\text{ }\mu\text{m}$, respectively.

understanding of polymer/solvent interactions is the total solubility parameter (δ); miscibility is improved when the components of a system have similar cohesive energy densities (E/V),⁵⁹ where the cohesive energy density is the energy required to infinitely separate a unit volume of a given species from its neighbors. The total solubility parameter (δ) can be described by three contributions of the Hansen solubility parameters (HSPs), namely, the dispersive (δ_D), the polar (δ_P), and H-bonding (δ_H) solubility parameters.^{41,60,61} The total solubility parameter (δ) is defined by eq 2,^{41,60}

$$\delta^2 = (E/V) = \delta_D^2 + \delta_P^2 + \delta_H^2 \quad (2)$$

where E is the cohesion energy or sum of the evaporation enthalpies, and V is the molar volume.

To systematically evaluate the solubility of P3HT in the solvent blends investigated here, the 3-dimensional Hansen space was explored. The three HSPs are used as Cartesian units and each solvent system can be represented by a coordinate. Solvents that effect polymer dissolution define the interaction radius (R_0) which determines the radius

of the sphere in Hansen space; solvents falling within R_0 dissolve the polymer, while the solvents outside of R_0 are not effective. The center of the sphere is determined by the polymer Hansen parameters. The distance between the polymer and solvent Hansen parameters is termed R_a , defined by eq 3,

$$R_a^2 = 4(\delta_{D1} - \delta_{D2})^2 + (\delta_{P1} - \delta_{P2})^2 + (\delta_{H1} - \delta_{H2})^2 \quad (3)$$

where subscripts 1 and 2 represent the solute and solvent, respectively. The relative energy difference ($\text{RED} = R_a/R_0$) provides an estimate of whether two materials will be miscible (miscible when $\text{RED} < 1$, partially miscible when $\text{RED} = 1$ and nonmiscible when $\text{RED} > 1$).

Abbott and Hansen software was used to determine HSPs for P3HT following methodology reported by Duong *et al.*,²⁶ and Brabec and co-workers.^{62,63} Good solvents, defined as solvents which can dissolve more than 5 mg/mL of the polymer, were assigned a value of "1", while poor solvents were assigned a value of "0". The solubility of P3HT in a variety of alternative solvents

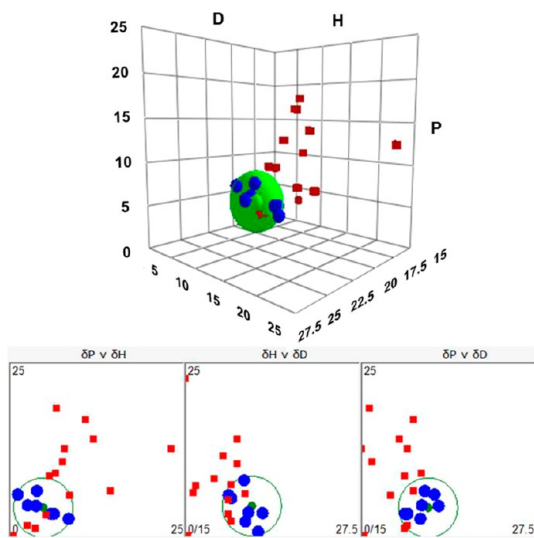


Figure 5. Hansen solubility parameter diagrams for P3HT and selected solvents. Solvents in blue are considered to be good solvents for P3HT while solvents in red are poor solvents.

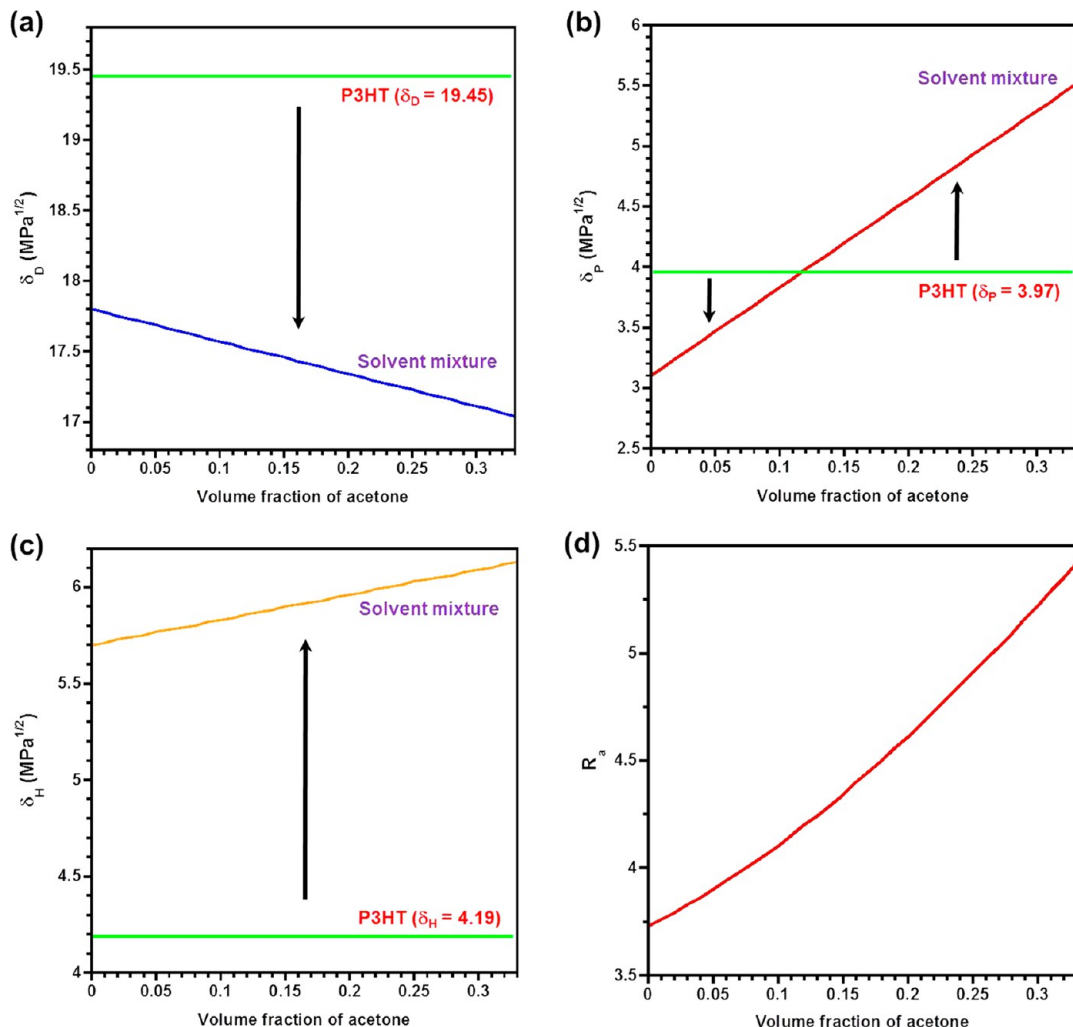


Figure 6. Hansen solubility parameters (a) δ_D , (b) δ_P and (c) δ_H of chloroform/acetone solvent blends and the distance (d) R_a between Hansen solubility parameters of P3HT and chloroform/acetone solvent as a function of acetone volume fraction; δ_D , δ_P and δ_H were numerically calculated by eq 4, and R_a was calculated using eq 3. Solubility parameters of pure solvents and P3HT are as follows; $\delta_D = 17.80$, $\delta_P = 3.10$ and $\delta_H = 5.70$ for chloroform; $\delta_D = 15.50$, $\delta_P = 10.40$ and $\delta_H = 7.00$ for acetone; and $\delta_D = 19.45$, $\delta_P = 3.97$ and $\delta_H = 4.19$ for P3HT.

is summarized in Supporting Information. The Hansen space creates the interaction radius, R_0 , for P3HT as shown in Figure 5, and also RED values of the solvents are obtained (see Supporting Information). Solvents in blue are considered to be good solvents for P3HT, while solvents in red are inferior/poor solvents. P3HT solubility parameters were calculated to be $\delta_D = 19.45 \text{ MPa}^{1/2}$, $\delta_P = 3.97 \text{ MPa}^{1/2}$ and $\delta_H = 4.19 \text{ MPa}^{1/2}$, with an interaction radius R_0 of $4.20 \text{ MPa}^{1/2}$.

Solvent solubility parameters were calculated as function of acetone volume fraction using eq 4,

$$\delta_x = \sum (\delta_x)_i \phi_i \quad (4)$$

where x represents D , P , or H , i stands for solvent species and ϕ_i refers to the volume fraction of component i . Calculated values of δ_D , δ_P and δ_H for the solvents as a function of acetone content are depicted in Figure 6. The range of 0 to 33 vol % acetone was examined because it is anticipated that the composition of the solvent will converge to a 33 vol % acetone

TABLE 1. Hansen Solubility Parameters of Chloroform/Acetone Blends Containing Different Proportions of Acetone

solvents	δ_D (MPa $^{1/2}$)	δ_P (MPa $^{1/2}$)	δ_H (MPa $^{1/2}$)
Chloroform	17.80	3.10	5.70
Acetone	15.50	10.40	7.00
Chloroform/acetone (v/v = 99.5/0.5)	17.79	3.14	5.71
Chloroform/acetone (v/v = 99.0/1.0)	17.78	3.17	5.71
Chloroform/acetone (v/v = 98.0/2.0)	17.75	3.25	5.73
Chloroform/acetone (v/v = 97.0/3.0)	17.73	3.32	5.74
Chloroform/acetone (v/v = 95.0/5.0)	17.69	3.47	5.77
Chloroform/acetone (v/v = 67.0/33.0)	17.04	5.51	6.13

solution during thin-film formation. As shown in Figure 6a, δ_D for chloroform/acetone decreases with an increase in acetone volume fraction. The difference between the P3HT and solvent values of δ_D increases with acetone incorporation, and thus in terms of δ_D , P3HT solubility in the solvent decreases. Examination of δ_P follows a different trend. The difference in δ_P between the polymer and the solvent increases with increasing acetone content up to a volume fraction of 0.12, but then decreases with increasing volume fraction of poor solvent up to 0.33 (Figure 6b). This trend indicates that with respect to δ_P , the polymer solubility initially increases with increasing acetone content, but once the volume fraction of poor solvent reaches 0.12, P3HT solubility decreases. Figure 6c shows that in terms of δ_H , the solubility of the polymer relative to the solvent decreases as the acetone content increases. Based upon eq 3, differences in δ_D dominate in the calculation of R_a , which increases with increased levels of the poor solvent, and polymer solubility decreases (Figure 6d). The solubility parameters of the solvent mixtures prepared with 0.5, 1, 2, 3, 5, and 33 vol % acetone are tabulated in Table 1 along with those of chloroform and acetone.

The RED of the solvents with respect to P3HT were calculated as a function of acetone volume fraction to understand how solubility of the polymer changes upon addition of acetone. As discerned from Figure 7a, the RED decreases with increasing acetone content. Thus, P3HT is expected to be soluble (> 5 mg/mL) when the volume fraction of acetone is less than 0.12, but become increasingly less soluble for volume fractions of acetone greater than 0.12. These results were experimentally verified: P3HT exhibited good solubility in solvents prepared with up to 10 vol % acetone, appearing bright orange with no apparent aggregation. Samples prepared with solvents containing 15–33 vol % acetone were poorly soluble and aggregation was readily apparent (Figure 7b).

Upon the basis of the solubility parameter analysis, the solubility of P3HT in chloroform/acetone solutions decreases during the thin-film solidification process; excess acetone and chloroform evaporate more quickly than the optimally hydrogen bonded system, allowing the acetone volume fraction to gradually

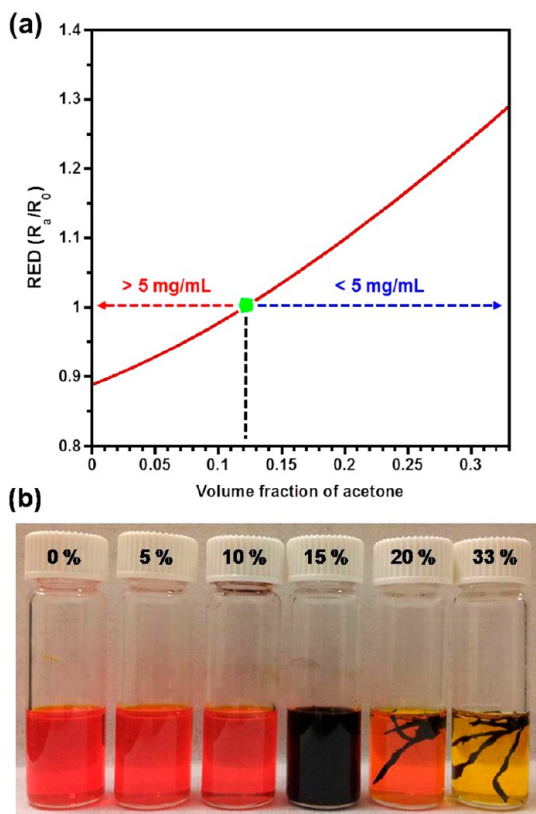
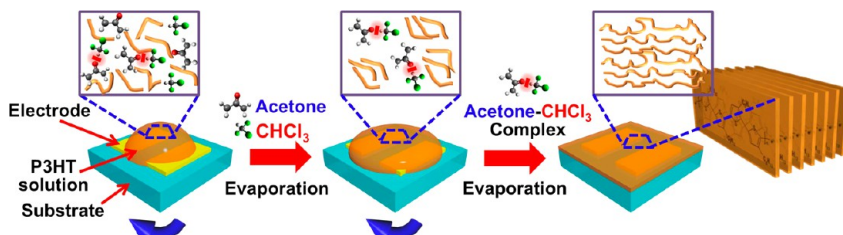


Figure 7. (a) Relative energy difference (RED) of chloroform/acetone solvent mixtures to P3HT, as a function of volume fraction of acetone and (b) photographs of P3HT solutions prepared with 5 mg/mL in various solvents (0, 5, 10, 15, 20, and 33 vol % acetone relative to chloroform). Solvent mixtures with RED less than 1 dissolve P3HT to a concentration more than 5 mg/mL and are considered to be good solvents, while solvent mixtures with RED more than 1 dissolve less than 5 mg/mL of polymer and are considered poor solvents.

increase up to approximately 33 vol %, regardless of the initial acetone volume fraction. Thus, as P3HT thin-film nanostructure initiates and evolves, the solvent system enhances molecular ordering between P3HT chains, with the degree of the molecular ordering being dependent upon the initial volume fraction of the poor solvent.

A mechanism to account for the observed enhanced supramolecular aggregation of P3HT chains during the deposition process is presented in Scheme 1. At the initial stages, acetone/chloroform solvent complexes formed via hydrogen bonding interactions exist alongside “free” acetone and chloroform in the P3HT precursor solutions. Supramolecular aggregation of the polymer is unfavorable because the overall solvent system represents a good solvent. As the film evolves, solvent molecules not involved in hydrogen bonding evaporate faster than their hydrogen bonded counterparts and as a result, the volume ratio of acetone to chloroform gradually increases up to approximately 33 vol %, while P3HT solubility commensurately decreases. Consequently, molecular ordering of the polymer



Scheme 1. A schematic illustration of the evolution of molecular ordering of P3HT chains during solvent evaporation.

chains improves due to a gradual transition from favorable to unfavorable solvent–solute interactions. The crystallinity of the films increases as well, however, the macroscopic field-effect mobility reaches a maximum at approximately 2 vol % acetone. At this point, even though crystallinity of resultant films continues to increase, other factors such as grain boundaries that negatively impact charge transport begin to predominate.

In addition to solvent–solute interactions, kinetic parameters associated with the coating process can impact molecular ordering, thin-film morphology and resultant polymer charge transport characteristics.^{21,64} To gain preliminary insight into the sensitivity of the system to kinetic parameters, the rate of solvent evaporation was varied through control of the spinning speed (see Supporting Information). Small differences in the optimum critical acetone concentration were observed; however, investigation into the kinetic processes associated with film formation and their impact on the morphology and charge transport characteristics of polymer based semiconductors will be required to elucidate the complicated relationships.

CONCLUSIONS

In conclusion, the macroscopic charge carrier transport characteristics of solution deposited P3HT thin-films can be enhanced simply by the addition of a small amount of a poor solvent that has a propensity to hydrogen bond. Specifically, addition of acetone to solutions of P3HT in chloroform affords improved molecular ordering of P3HT chains, resulting in enhanced macroscopic charge transport characteristics of resultant thin films. The two-dimensional molecular ordering of the polymer film was controlled by varying the amount of poor solvent added to a precursor solution, and a correlation between the field-effect mobility and molecular ordering of the π -conjugated polymer chains was investigated. During film formation, the relative volume fraction of poor to good

solvent gradually increased due to hydrogen bonding interactions between the constituent solvent molecules. Hansen solubility parameters of the polymer and solvent blends were employed to systematically understand how the solvent mixtures can enhance the supramolecular assembly of polymer chains during deposition and subsequently impact the electrical performance of the thin P3HT films. The solubility threshold of P3HT appeared at an acetone volume fraction of 0.12 relative to the majority solvent, chloroform, and the RED value of the solvent to P3HT varied from less than to greater than 1 during film formation, indicating that the solvent characteristics change from those of a good solvent to those of a poor solvent. This shift in solvent characteristics to a system that presents unfavorable solvent–solute interactions enhances the proportion of well-ordered molecular π – π stacked P3HT chains. These studies provided for a mechanistic illustration of the polymer molecular ordering process during film formation.

This simple solvent based hydrogen bonding assisted process represents a benign alternative for enhancing ordered, aggregated π -conjugated semiconducting polymer architectures. The approach that utilizes both solvent–solvent and solvent–solute interactions, as determined through spectroscopic and solubility parameter analysis, could prove attractive in the pursuit of robust, low-cost, large-area electronic device fabrication methodologies. Further, the spectrum of solvent systems applicable to polymer semiconductor device fabrication may be expanded, enabling facile processing of organic–organic blends or organic–inorganic composites. The mechanistic approach, employing Hansen solubility parameters, used to define a solvent system contributes to understanding the evolution of macroscopic polymer thin-film morphology and charge transport characteristics for a variety of applications including chemical sensors, OFETs, light emitting diodes and organic photovoltaic cells.

MATERIALS AND METHODS

Materials. P3HT (catalog no. 445703), chloroform (HPLC grade), acetone (HPLC grade), chlorobenzene (HPLC grade) and 2,3-dimethylbutane (analytical standard grade) were purchased from Sigma Aldrich and used without further purification. The P3HT used in this study had a M_n of 40.3 kDa and M_w of 91.4 kDa

with respect to polystyrene standards as determined by Gel Permeation Chromatography (Waters 1515 Isocratic HPLC equipped with a Waters 2489 UV/vis detector and Styragel HR 5E column) using tetrahydrofuran as the eluent. All data were processed using Breeze 2 software. The head to tail regioregularity (RR) was estimated to be approximately 92%

(Bruker DSX 300 ^1H NMR in deuterated chloroform solution at 293 K).

Organic Field-Effect Transistor (OFET) Fabrication and Characterization.

Two contact FET devices were prepared *via* spin coating the relevant P3HT solution onto a 300 nm thick SiO_2 gate dielectric. The highly doped silicon wafer served as the gate electrode, while Au/Cr was used for the source and drain contacts. The source and drain contacts were fabricated using a standard photolithography based lift-off process, followed by E-beam evaporation (Denton Explorer) of 50 nm Au contacts with 3 nm of Cr as the adhesion layer. Before spin coating P3HT solutions, all devices were cleaned for 15 min in a UV-ozone cleaner (Novascan PSD-UV) to ensure complete removal of any residual photoresist and other organic contaminants. In a typical preparation of the polymer solutions, 15 mg of P3HT was introduced into 3 mL of relevant solvent mixtures containing small amount of poor solvent (0, 0.5, 1, 2, 3, and 5 vol %) in air. Subsequently, the solutions were stirred in a sealed vial for at least 30 min at *ca.* 60 °C. OFETs were prepared by spin coating (WS-650MZ-23NPP, Laurell) the solutions onto precleaned substrates at a spin speed of 1500 rpm for 60 s in air, and tested in a nitrogen ambient using an Agilent 4155C semiconductor parameter analyzer.

UV–Vis Spectroscopy. The solution and solid state UV–vis spectra were recorded using an Agilent 8510 UV–vis spectrophotometer. Films for solid state studies were prepared by spin coating the requisite solution onto precleaned glass slides following the same procedures used to prepare OFET devices.

Grazing Incidence X-ray Diffraction (GIXD). Out-of-plane grazing incidence X-ray diffraction data were obtained using a Panalytical X'Pert Pro system equipped with a Cu X-ray source operating at 45 kV and 40 mA. The grazing incidence angle was fixed at 0.2° and the detector was scanned from 3° to 30°. Peak positions were obtained from the measured profiles by fitting the peaks using the analysis software (MDI JADE). For the preparation of samples for GIXD measurements, P3HT solutions were spin coated onto hydrophilic silicon substrates with native oxide that were cleaned using the procedure employed for fabrication of bottom contact FET devices. The spin coating procedures and solutions were identical to those used for fabrication of OFET devices.

Atomic Force Microscopy (AFM). The AFM measurements were performed on films spin coated onto bottom contact OFET substrates using a Veeco Digital Instruments Dimension 3100 scanning probe microscope operating in tapping mode with a silicon tip (NSC14, Mikro Masch).

Hansen Solubility Parameter Characterization. P3HT (1, 5, and/or 10 mg/mL) was mixed with 3 mL of solvent as per the defined procedure for solubility parameter determination (a list of solvents examined in this study are presented in Table S1 in Supporting Information) and heated at 60 °C for at least 3 h. Subsequently, the solutions were cooled to ambient temperature where they remained for 6 h. The solubility parameters were determined from these solutions *via* visual examination. Solvents were categorized as poor if they were unable to dissolve more than 5 mg of P3HT/mL of solvent and good if they were able to dissolve more than 5 mg of polymer/mL of solvent. For the purposes of Hansen solubility parameter (HSP) analysis using requisite software (Hansen Solubility Parameters in Practice third edition), a poor solvent was assigned a value of "0" and good solvent was assigned a value of "1". The HSP software package creates a sphere in Hansen space based on the coordinates of the good solvents, while excluding those of the poor solvents. The center of the sphere represents the HSPs for P3HT. The fitting accuracy appeared with a value of "1", indicating the best fit. The value is determined by the program which evaluates the input data using a quality of fit function.⁶⁵ Supporting Information Table S1 summarizes the solubility results of P3HT in the organic solvents evaluated here, and Supporting Information Table S2 presents the HSPs for the solvents along with values of their relative energy difference (RED) to P3HT.

Conflict of Interest: The authors declare no competing financial interest.

Acknowledgment. The financial support of the Georgia Institute of Technology and the Air Force Office of Scientific

Research (FA9550-12-1-0248) is gratefully acknowledged. The authors would also like to thank H. Li for useful discussions relating to hydrogen bonding.

Supporting Information Available: UV–vis spectra of P3HT in chlorobenzene/acetone and chloroform/2,3-dimethylbutane solutions and corresponding P3HT films obtained by spin coating; GIXD profiles and AFM images of the P3HT films; evaporation rate of chloroform/acetone, chlorobenzene/acetone and chloroform/2,3-dimethylbutane as a function of poor solvent volume ratio from P3HT solutions and FT-IR spectra of P3HT in corresponding solvent mixtures; field-effect mobilities of P3HT films obtained *via* spin coating with different spinning speeds from chloroform/acetone solutions; solubility of P3HT in selected organic solvents; solubility parameters of selected organic solvents and their RED to P3HT. This material is available free of charge *via* the Internet at <http://pubs.acs.org>.

REFERENCES AND NOTES

- Gustafsson, G.; Cao, Y.; Treacy, G. M.; Klavetter, F.; Colaneri, N.; Heeger, A. J. Flexible Light-Emitting-Diodes Made from Soluble Conducting Polymers. *Nature* **1992**, *357*, 477–479.
- Bao, Z. N.; Lovinger, A. J. Soluble Regioregular Polythiophene Derivatives as Semiconducting Materials for Field-Effect Transistors. *Chem. Mater.* **1999**, *11*, 2607–2612.
- Lee, K. H.; Schwenn, P. E.; Smith, A. R. G.; Cavaye, H.; Shaw, P. E.; James, M.; Krueger, K. B.; Gentle, I. R.; Meredith, P.; Burn, P. L. Morphology of All-Solution-Processed "Bilayer" Organic Solar Cells. *Adv. Mater.* **2011**, *23*, 766–770.
- Gaynor, W.; Lee, J. Y.; Peumans, P. Fully Solution-Processed Inverted Polymer Solar Cells with Laminated Nanowire Electrodes. *ACS Nano* **2010**, *4*, 30–34.
- Zhuang, X. D.; Chen, Y.; Liu, G.; Li, P. P.; Zhu, C. X.; Kang, E. T.; Neoh, K. G.; Zhang, B.; Zhu, J. H.; Li, Y. X. Conjugated-Polymer-Functionalized Graphene Oxide: Synthesis and Nonvolatile Rewritable Memory Effect. *Adv. Mater.* **2010**, *22*, 1731–1735.
- Lobez, J. M.; Andrew, T. L.; Bulovic, V.; Swager, T. M. Improving the Performance of P3HT:Fullerene Solar Cells with Side-Chain-Functionalized Poly(thiophene) Additives: A New Paradigm for Polymer Design. *ACS Nano* **2012**, *6*, 3044–3056.
- Coropceanu, V.; Cornil, J.; da Silva, D. A.; Olivier, Y.; Silbey, R.; Bredas, J. L. Charge Transport in Organic Semiconductors. *Chem. Rev.* **2007**, *107*, 926–952.
- Street, R. A.; Northrup, J. E.; Salleo, A. Transport in Polycrystalline Polymer Thin-Film Transistors. *Phys. Rev. B* **2005**, *71*, 165202.
- Goffri, S.; Muller, C.; Stigelin-Stutzmann, N.; Breiby, D. W.; Radano, C. P.; Andreasen, J. W.; Thompson, R.; Janssen, R. A. J.; Nielsen, M. M.; Smith, P.; et al. Multicomponent Semiconducting Polymer Systems with Low Crystallization-Induced Percolation Threshold. *Nat. Mater.* **2006**, *5*, 950–956.
- Chen, D.; Zhao, W.; Russell, T. P. P3HT Nanopillars for Organic Photovoltaic Devices Nanoimprinted by AAO Templates. *ACS Nano* **2012**, *6*, 1479–1485.
- Sirringhaus, H.; Brown, P. J.; Friend, R. H.; Nielsen, M. M.; Bechgaard, K.; Langeveld-Voss, B. M. W.; Spiering, A. J. H.; Janssen, R. A. J.; Meijer, E. W.; Herwig, P.; et al. Two-Dimensional Charge Transport in Self-Organized, High-Mobility Conjugated Polymers. *Nature* **1999**, *401*, 685–688.
- Hill, C. M.; Zhu, Y.; Pan, S. Fluorescence and Electroluminescence Quenching Evidence of Interfacial Charge Transfer in Poly(3-hexylthiophene): Graphene Oxide Bulk Heterojunction Photovoltaic Devices. *ACS Nano* **2011**, *5*, 942–951.
- Cho, S.; Lee, K.; Yuen, J.; Wang, G. M.; Moses, D.; Heeger, A. J.; Surin, M.; Lazzaroni, R. Thermal Annealing-Induced Enhancement of the Field-Effect Mobility of Regioregular Poly(3-hexylthiophene) Films. *J. Appl. Phys.* **2006**, *100*, 114503.
- Yang, H. C.; Shin, T. J.; Yang, L.; Cho, K.; Ryu, C. Y.; Bao, Z. N. Effect of Mesoscale Crystalline Structure on the Field-Effect Mobility of Regioregular Poly(3-hexylthiophene) in Thin-Film Transistors. *Adv. Funct. Mater.* **2005**, *15*, 671–676.

15. Park, Y. D.; Lee, H. S.; Choi, Y. J.; Kwak, D.; Cho, J. H.; Lee, S.; Cho, K. Solubility-Induced Ordered Polythiophene Precursors for High-Performance Organic Thin-Film Transistors. *Adv. Funct. Mater.* **2009**, *19*, 1200–1206.
16. Aiyar, A. R.; Hong, J. I.; Reichmanis, E. Regioregularity and Intrachain Ordering: Impact on the Nanostructure and Charge Transport in Two-Dimensional Assemblies of Poly(3-hexylthiophene). *Chem. Mater.* **2012**, *24*, 2845–2853.
17. Chen, D. A.; Nakahara, A.; Wei, D. G.; Nordlund, D.; Russell, T. P. P3HT/PCBM Bulk Heterojunction Organic Photovoltaics: Correlating Efficiency and Morphology. *Nano Lett.* **2011**, *11*, 561–567.
18. Kline, R. J.; McGehee, M. D.; Kadnikova, E. N.; Liu, J. S.; Frechet, J. M. J. Controlling the Field-Effect Mobility of Regioregular Polythiophene by Changing the Molecular Weight. *Adv. Mater.* **2003**, *15*, 1519–1522.
19. Kline, R. J.; McGehee, M. D.; Kadnikova, E. N.; Liu, J. S.; Frechet, J. M. J.; Toney, M. F. Dependence of Regioregular Poly(3-hexylthiophene) Film Morphology and Field-Effect Mobility on Molecular Weight. *Macromolecules* **2005**, *38*, 3312–3319.
20. Zhang, R.; Li, B.; Iovu, M. C.; Jeffries-EL, M.; Sauve, G.; Cooper, J.; Jia, S. J.; Tristram-Nagle, S.; Smilgies, D. M.; Lambeth, D. N.; et al. Nanostructure Dependence of Field-Effect Mobility in Regioregular Poly(3-hexylthiophene) Thin Film Field Effect Transistors. *J. Am. Chem. Soc.* **2006**, *128*, 3480–3481.
21. Aiyar, A. R.; Hong, J. I.; Nambiar, R.; Collard, D. M.; Reichmanis, E. Tunable Crystallinity in Regioregular Poly(3-Hexylthiophene) Thin Films and Its Impact on Field Effect Mobility. *Adv. Funct. Mater.* **2011**, *21*, 2652–2659.
22. Xiao, X. L.; Hu, Z. J.; Wang, Z. B.; He, T. B. Study on the Single Crystals of Poly(3-octylthiophene) Induced by Solvent-Vapor Annealing. *J. Phys. Chem. B* **2009**, *113*, 14604–14610.
23. Fu, Y.; Lin, C.; Tsai, F. Y. High Field-Effect Mobility from Poly(3-hexylthiophene) Thin-Film Transistors by Solvent-Vapor-Induced Reflow. *Org. Electron.* **2009**, *10*, 883–888.
24. Kim, B. G.; Kim, M. S.; Kim, J. Ultrasonic-Assisted Nanodimensional Self-Assembly of Poly-3-hexylthiophene for Organic Photovoltaic Cells. *ACS Nano* **2010**, *4*, 2160–2166.
25. Park, J. H.; Kim, J. S.; Lee, J. H.; Lee, W. H.; Cho, K. Effect of Annealing Solvent Solubility on the Performance of Poly(3-hexylthiophene)/Methanofullerene Solar Cells. *J. Phys. Chem. C* **2009**, *113*, 17579–17584.
26. Duong, D. T.; Walker, B.; Lin, J.; Kim, C.; Love, J.; Purushothaman, B.; Anthony, J. E.; Nguyen, T. Q. Molecular Solubility and Hansen Solubility Parameters for the Analysis of Phase Separation in Bulk Heterojunctions. *J. Polym. Sci., Part B: Polym. Phys.* **2012**, *50*, 1405–1413.
27. Chang, J. F.; Sun, B. Q.; Breiby, D. W.; Nielsen, M. M.; Solling, T. I.; Giles, M.; McCulloch, I.; Sirringhaus, H. Enhanced Mobility of Poly(3-hexylthiophene) Transistors by Spin-Coating from High-Boiling-Point Solvents. *Chem. Mater.* **2004**, *16*, 4772–4776.
28. Hidber, P. C.; Nealey, P. F.; Helbig, W.; Whitesides, G. M. New Strategy for Controlling the Size and Shape of Metallic Features Formed by Electroless Deposition of Copper: Micro-contact Printing of Catalysts on Oriented Polymers, Followed by Thermal Shrinkage. *Langmuir* **1996**, *12*, 5209–5215.
29. Hyun, D. C.; Jeong, U. Substrate Thickness: An Effective Control Parameter for Polymer Thin Film Buckling on PDMS Substrates. *J. Appl. Polym. Sci.* **2009**, *112*, 2683–2690.
30. Pandey, S. S.; Gerard, M.; Sharma, A. L.; Malhotra, B. D. Thermal Analysis of Chemically Synthesized Polyemeraldine Base. *J. Appl. Polym. Sci.* **2000**, *75*, 149–155.
31. Henderson, R. K.; Jimenez-Gonzalez, C.; Constable, D. J. C.; Alston, S. R.; Inglis, G. G. A.; Fisher, G.; Sherwood, J.; Binks, S. P.; Curzons, A. D. Expanding GSK's Solvent Selection Guide - Embedding Sustainability into Solvent Selection Starting at Medicinal Chemistry. *Green Chem.* **2011**, *13*, 854–862.
32. Kiriy, N.; Jahne, E.; Adler, H. J.; Schneider, M.; Kiriy, A.; Gorodyska, G.; Minko, S.; Jahnichen, D.; Simon, P.; Fokin, A. A.; et al. One-Dimensional Aggregation of Regioregular Polyalkylthiophenes. *Nano Lett.* **2003**, *3*, 707–712.
33. Moule, A. J.; Meerholz, K. Controlling Morphology in Polymer-Fullerene Mixtures. *Adv. Mater.* **2008**, *20*, 240–245.
34. Li, L. G.; Lu, G. H.; Yang, X. N. Improving Performance of Polymer Photovoltaic Devices Using an Annealing-Free Approach via Construction of Ordered Aggregates in Solution. *J. Mater. Chem.* **2008**, *18*, 1984–1990.
35. O'Neill, A.; Khan, U.; Nirmalraj, P. N.; Boland, J.; Coleman, J. N. Graphene Dispersion and Exfoliation in Low Boiling Point Solvents. *J. Phys. Chem. C* **2011**, *115*, 5422–5428.
36. Hernandez, Y.; Nicolosi, V.; Lotya, M.; Blighe, F. M.; Sun, Z. Y.; De, S.; McGovern, I. T.; Holland, B.; Byrne, M.; Gun'ko, Y. K.; et al. High-Yield Production of Graphene by Liquid-Phase Exfoliation of Graphite. *Nat. Nanotechnol.* **2008**, *3*, 563–568.
37. Zhang, X. Y.; Coleman, A. C.; Katsonis, N.; Browne, W. R.; van Wees, B. J.; Feringa, B. L. Dispersion of Graphene in Ethanol Using a Simple Solvent Exchange Method. *Chem. Commun.* **2010**, *46*, 7539–7541.
38. He, M.; Ge, J.; Fang, M.; Qiu, F.; Yang, Y. L. Fabricating Polythiophene into Highly Aligned Microwire Film by Fast Evaporation of Its Whisker Solution. *Polymer* **2010**, *51*, 2236–2243.
39. Kim, J. S.; Lee, J. H.; Park, J. H.; Shim, C.; Sim, M.; Cho, K. High-Efficiency Organic Solar Cells Based on Preformed Poly(3-hexylthiophene) Nanowires. *Adv. Funct. Mater.* **2011**, *21*, 480–486.
40. Yang, H. H.; LeFevre, S. W.; Ryu, C. Y.; Bao, Z. N. Solubility-Driven Thin Film Structures of Regioregular Poly(3-hexylthiophene) Using Volatile Solvents. *Appl. Phys. Lett.* **2007**, *90*, 172116.
41. Abbott, S. J.; Hansen, C. M. Hansen Solubility Parameters in Practice (software), www.hansen-solubility.com, (accessed November 2012).
42. Choi, K.; Tedder, D. W. Molecular Interactions in Chloroform-Diluent Mixtures. *AIChE J.* **1997**, *43*, 196–211.
43. Vargas, R.; Garza, J.; Dixon, D. A.; Hay, B. P. How Strong Is the C^o-H^o=C Hydrogen Bond?. *J. Am. Chem. Soc.* **2000**, *122*, 4750–4755.
44. Xu, Z.; Li, H. R.; Wang, C. M. Can a Blue Shift of the C-H Stretching Modes of Inactivated C Groups be an Indicator of Weak C-H^oO Hydrogen Bonds?. *ChemPhysChem* **2006**, *7*, 2460–2463.
45. Solomonov, B. N.; Varfolomeev, M. A.; Abaidullina, D. I. Cooperative Hydrogen Bonding in Solution: Influence of Molecule Structure. *Vib. Spectrosc.* **2007**, *43*, 380–386.
46. Vaz, P. D.; Nolasco, M. M.; Gil, F. P. S. C.; Ribeiro-Claro, P. J. A.; Tomkinson, J. Hydrogen-Bond Dynamics of C-H^oO Interactions: The Chloroform-Acetone Case. *Chem. -Eur. J.* **2010**, *16*, 9010–9017.
47. Horowitz, G. Organic Field-Effect Transistors. *Adv. Mater.* **1998**, *10*, 365–377.
48. Jia, H. P.; Gowrisanker, S.; Pant, G. K.; Wallace, R. M.; Gnade, B. E. Effect of Poly (3-hexylthiophene) Film Thickness on Organic Thin Film Transistor Properties. *J. Vac. Sci. Technol., A* **2006**, *24*, 1228–1232.
49. Chua, L. L.; Zaumseil, J.; Chang, J. F.; Ou, E. C. W.; Ho, P. K. H.; Sirringhaus, H.; Friend, R. H. General Observation of n-Type Field-Effect Behaviour in Organic Semiconductors. *Nature* **2005**, *434*, 194–199.
50. Berson, S.; De Bettignies, R.; Baily, S.; Guillerez, S. Poly(3-hexylthiophene) Fibers for Photovoltaic Applications. *Adv. Funct. Mater.* **2007**, *17*, 1377–1384.
51. Gurau, M. C.; Delongchamp, D. M.; Vogel, B. M.; Lin, E. K.; Fischer, D. A.; Sambasivan, S.; Richter, L. J. Measuring Molecular Order in Poly(3-alkylthiophene) Thin Films with Polarizing Spectroscopies. *Langmuir* **2007**, *23*, 834–842.
52. Brown, P. J.; Thomas, D. S.; Kohler, A.; Wilson, J. S.; Kim, J. S.; Ramsdale, C. M.; Sirringhaus, H.; Friend, R. H. Effect of Interchain Interactions on the Absorption and Emission of Poly(3-hexylthiophene). *Phys. Rev. B* **2003**, *67*, 064203.
53. McCulloch, I.; Heeney, M.; Bailey, C.; Genevicius, K.; I, M.; Shkunov, M.; Sparrowe, D.; Tierney, S.; Wagner, R.; Zhang, W. M.; et al. Liquid-Crystalline Semiconducting Polymers with High Charge-Carrier Mobility. *Nat. Mater.* **2006**, *5*, 328–333.

54. Prosa, T. J.; Winokur, M. J.; Moulton, J.; Smith, P.; Heeger, A. J. X-Ray Structural Studies of Poly(3-alkylthiophenes): An Example of an Inverse Comb. *Macromolecules* **1992**, *25*, 4364–4372.
55. Kline, R. J.; McGehee, M. D.; Toney, M. F. Highly Oriented Crystals at the Buried Interface in Polythiophene Thin-Film Transistors. *Nat. Mater.* **2006**, *5*, 222–228.
56. Yamamoto, T.; Komarudin, D.; Arai, M.; Lee, B. L.; Suganuma, H.; Asakawa, N.; Inoue, Y.; Kubota, K.; Sasaki, S.; Fukuda, T.; et al. Extensive Studies on pi-Stacking of Poly(3-alkylthiophene-2,5-diyl)s and Poly(4-alkylthiazole-2,5-diyl)s by Optical Spectroscopy, NMR Analysis, Light Scattering Analysis, and X-Ray Crystallography. *J. Am. Chem. Soc.* **1998**, *120*, 2047–2058.
57. Zhang, X. K. K.; Lewars, E. G.; March, R. E.; Parnis, J. M. Vibrational-Spectrum of the Acetone-Water Complex: A Matrix-Isolation FTIR and Theoretical Study. *J. Phys. Chem.* **1993**, *97*, 4320–4325.
58. Tummala, N. R.; Striolo, A. Hydrogen-Bond Dynamics for Water Confined in Carbon Tetrachloride-Acetone Mixtures. *J. Phys. Chem. B* **2008**, *112*, 10675–10683.
59. Hildebrand, J. H.; Scott, R. L. The Entropy of Solution of Nonelectrolytes. *J. Chem. Phys.* **1952**, *20*, 1520–1521.
60. Hansen, C. M.; Smith, A. L. Using Hansen Solubility Parameters to Correlate Solubility of C-60 Fullerene in Organic Solvents and in Polymers. *Carbon* **2004**, *42*, 1591–1597.
61. Hansen, C. M. *Hansen Solubility Parameters: A User's Handbook*, 2nd ed.; CRC Press: Boca Raton, FL, 2007; pp 1–24.
62. Machui, F.; Langner, S.; Zhu, X. D.; Abbott, S.; Brabec, C. J. Determination of the P3HT:PCBM Solubility Parameters via a Binary Solvent Gradient Method: Impact of Solubility on the Photovoltaic Performance. *Sol. Energy Mater. Sol. Cells* **2012**, *100*, 138–146.
63. Machui, F.; Abbott, S.; Waller, D.; Koppe, M.; Brabec, C. J. Determination of Solubility Parameters for Organic Semiconductor Formulations. *Macromol. Chem. Phys.* **2011**, *212*, 2159–2165.
64. Aiyar, A.; Hong, J.-I.; Izumi, J.; Choi, D.; Kleinhenz, N.; Reichmanis, E. Ultrasound-Induced Ordering in Poly (3-hexylthiophene): Role of Molecular and Process Parameters on Morphology and Charge Transport. *ACS Appl. Mater. Interfaces* **2013**, *5*, 2368–2377.
65. Yao, Y.; Hou, J. H.; Xu, Z.; Li, G.; Yang, Y. Effect of Solvent Mixture on the Nanoscale Phase Separation in Polymer Solar Cells. *Adv. Funct. Mater.* **2008**, *18*, 1783–1789.